Russian Journal of Bioorganic Chemistry, Vol. 29, No. 5, 2003, pp. 426–433. Translated from Bioorganicheskaya Khimiya, Vol. 29, No. 5, 2003, pp. 470–478.

Structural and Functional Peculiarities of Homologous Domains of Angiotensin-Converting Enzyme

S. V. Voronov, P. V. Binevski, N. A. Zueva, V. A. Palyulin, I. I. Baskin, M. A. Orlova, and O. A. Kost[1]

Faculty of Chemistry, Moscow State University, Vorob'evy gory, Moscow, 119992 Russia

Received December 20, 2002; in final form, January 22, 2003

Abstract—Somatic angiotensin-converting enzyme (ACE) consists of two homologous domains, each of them containing an active site. Differences in substrate specificities and affinity to inhibitors of the active sites of the two domains of bovine ACE are described. The ACE domains demonstrate different thermostability, and the reasons for this difference are analyzed. A structural model of the ACE domains is suggested, which allows us to reveal the structural subdomain important for the protein stability and localize the hydrophobic and carbohydrate-binding sites.

Key words: *angiotensin-converting enzyme, secondary structure, three-dimensional structure; 8-anilino-1-naphthalenesulfonic acid; thermal inactivation; γ-inactivation*

INTRODUCTION

Angiotensin-converting enzyme (peptidyldipeptidase A, EC 3.4.15.1) is a zinc-containing metalloprotease, which consists of 1277 amino acid residues and belongs to the zincin class.[2] The unique feature of the enzyme molecule synthesized in somatic cells is the presence of two highly homologous domains within a single polypeptide chain, each domain containing its own active site [1]. These domains are called as *N*-domain and *C*-domain according to their location in the polypeptide chain. Their homology is as high as 67–73% (depending on an organism), and the identity of amino acid residues in their central parts containing the zinc-binding motifs reaches 89% [2]. At the same time, both domains themselves and their active sites are not identical. For example, the *N*-terminal domain of human ACE was shown to be much more glycosylated than its *C*-domain [3]. In the experiments with mutant forms of human ACE, the recombinant *N*-domain was found to be more stable at high temperatures than the *C*-domain or the two-domain form of ACE [4]. Similar results were also obtained for the bovine ACE by the method of differential scanning calorimetry. The somatic enzyme had two peaks of thermal absorption at 55 and 70°C, whereas the individual *N*-domain of ACE prepared by a limited proteolysis of the parent somatic form exhibited only one high-temperature peak [5]. The *N*-domain is also more stable toward the action of urea and the extreme pH values [6].

The three-dimensional structure of the full-size ACE and its domains is still not determined, and the structural backgrounds of the functional peculiarities of ACE domains are unknown.

The ACE catalytic sites hydrolyze the same peptide substrates and bind the same inhibitors. However, these sites are distinguished in the rate of the peptide hydrolysis, efficiency of the inhibitor binding, and the profile of activation by chloride anions [2]. It has previously been assumed that catalytic hydrolysis proceeded independently on the two ACE active sites [7]. However, some information now appeared that the active sites of the enzyme interact with each other [6, 8, 9], which implies a spatial proximity and contacts between the domains.

In this study, we present for the first time the information on the substrate specificity of bovine ACE and the affinity of its active sites to the inhibitors, on the different stability of its two enzymic domains and its possible reasons, and suggest a structural model of the ACE domains.

RESULTS AND DISCUSSION

It is known that a partial denaturation of the somatic enzyme results in the denaturation of its *C*-domain, whereas the *N*-domain preserves its catalytic activity and can be isolated in the individual form after the limited proteolysis of the denatured protein [10]. The bovine testicular enzyme was used as an individual *C*-domain. This enzyme is identical to the *C*-domain of the somatic ACE except for short *N*-terminal sequence that does not influence the enzyme catalytic

[1] Corresponding author; fax: +7 (095) 939-5417; e-mail: kost@enzyme.chem.msu.ru

[2] Abbreviations: ACE, angiotensin-converting enzyme; ANS, 8-anilino-1-naphthalenesulfonic acid; and FA, 2-furylacryloyl.

1068-1620/03/2905-0426$25.00

Table 1. Kinetic parameters of the hydrolysis of the synthetic tripeptide substrates by the single-domain forms of the bovine ACE*

Substrate	*N*-domain of ACE		Testicular ACE	
	k_{cat}, s^{-1}	K_m, mM	k_{cat}, s^{-1}	K_m, mM
FA-Phe-Gly-Gly	279 ± 10	1.40 ± 0.02	260 ± 14	0.50 ± 0.02
Hip-His-Leu	12 ± 1	0.50 ± 0.05	12 ± 1	0.60 ± 0.03
Cbz-Phe-His-Leu	122 ± 10	0.15 ± 0.02	19 ± 2	0.13 ± 0.02
FA-Phe-Ala-Ala	35 ± 3	0.05 ± 0.02	178 ± 15	0.05 ± 0.01
FA-Phe-Ala-Lys	35 ± 3	0.14 ± 0.01	85 ± 7	0.17 ± 0.02
FA-Phe-Phe-Arg	45 ± 4	0.05 ± 0.01	76 ± 8	0.12 ± 0.02

*The substrates were hydrolyzed in 50 mM Hepes buffer (pH 7.5) containing 150 mM NaCl and 1 μM $ZnCl_2$ at 25°C.

functions [11]. Thus, we could compare the catalytic functions of two individual domains of bovine ACE.

Kinetic parameters of the hydrolysis of synthetic tripeptide substrates by the individual active sites of bovine ACE are given in Table 1. It was found that a number of substrates were equally hydrolyzed on both active sites of bovine enzyme (for comparison note that the *C*-domain of human ACE hydrolyzes Hip-His-Leu substrate nine times faster than the *N*-domain [7]). The substrates FA-Phe-Ala-Ala, FA-Phe-Ala-Lys and FA-Phe-Ala-Arg were faster hydrolyzed by the *C*-domain (differences in the values of the catalytic constants along with the similar values of the Michaelis constants), but Cbz-Phe-His-Leu was faster hydrolyzed on the *N*-domain of ACE (whereas the human ACE hydrolyzed this substrate with the practically equal rate on both sites [12]). As a whole, these data agree with the earlier proposal [7, 13] about lesser demands of the *C*-domain active site to the structure of substrate.

The efficiencies of inhibition of both active sites of bovine ACE by the reversible competitive inhibitors are given in Table 2. The only significant difference in the values of inhibition constants was observed for captopril that more effectively inhibited the *N*-domain of the enzyme as in the case of human ACE [14].

Thus, the bovine ACE active sites somewhat differ in their substrate specificity and in their affinity to inhibitors, and this differences does not coincide with those previously revealed for the active sites of the human enzyme.

Functional difference between the enzyme domains is also revealed when comparing their stability. The kinetics of the irreversible thermal denaturation of the two-domain somatic ACE has a pronounced two-phase character (Fig. 1a), which does not depend on the protein concentration and suggests the presence in the system of at least two fractions with different stability. The rate constant of the thermal denaturation of the testicular ACE coincided with that of the labile fraction, whereas the stable fraction was denatured with the same rate constant as the isolated individual *N*-domain. The results allowed analysis of the kinetics of the thermal denaturation of the somatic ACE in a wide range of temperatures and the determination of the values of activation energy for the denaturation of each domain in the enzyme. The data are plotted in the Arrhenius coordinates in Fig. 1b. A more than double difference in the E_a values illustrates the difference in thermostability of the homologous domains of ACE.

It is important that the different thermostability of the domains opens a possibility for the selective denaturation of one of the domains (*C*-domain) with the formation of the catalytically active individual *N*-domain (after proteolysis) or the *N*-domain within the full-size enzyme with the denatured *C*-domain; in this case, the presence of denatured *C*-domain had no effect either on the stability or on the catalytic functions of the *N*-domain [5]. Thus, we can conclude that the domains in the molecule of somatic ACE are denatured independently of each other, which suggests that the spatial structures of these domains are also independent.

A higher stability of the ACE *N*-domain was also demonstrated in the experiments of the enzyme denaturation by action of the products of water radiolysis with γ-irradiation. In contrast to the heat treatment that involves the whole volume of the molecule, the products of water radiolysis mainly react with the protein surface [15]. It was found that the individual *N*-domain

Table 2. Inhibition constants of hydrolysis of Cbz-Phe-His-Leu by single-domain ACE forms by competitive inhibitors

Inhibitor	K_i, M	
	N-domain	testicular ACE
Lisinopril	$(2.0 \pm 0.1) \times 10^{-10}$	$(1.2 \pm 0.2) \times 10^{-10}$
Captopril	$(5.0 \pm 0.2) \times 10^{-10}$	$(9.1 \pm 0.9) \times 10^{-9}$
PP-09	$(1.5 \pm 0.2) \times 10^{-8}$	$(4.7 \pm 0.4) \times 10^{-8}$
Enalapril maleate	$(8.6 \pm 0.4) \times 10^{-8}$	$(2.6 \pm 0.1) \times 10^{-7}$

Note: The hydrolysis was performed in 50 mM Hepes buffer (pH 7.5) containing 150 mM NaCl and 1 μM $ZnCl_2$ at 37°C.

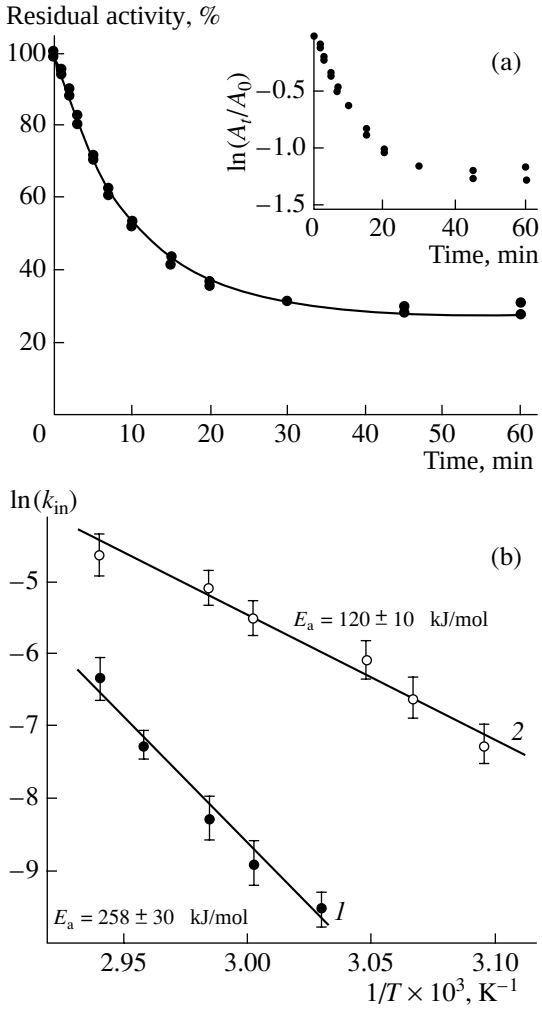

Fig. 1. The thermal inactivation of somatic ACE: (a) kinetics of the thermal inactivation of ACE at 55°C (in the insert, the same data plotted in the semi-logarithmic coordinates); (b) temperature dependence of the denaturation constants of (*1*) *N*-domain and (*2*) *C*-domain of the somatic ACE in the mixture of 0.025 M phosphate–0.025 M borate buffer (pH 6.5) containing 0.15 M NaCl and 1 μM Zn^{2+}, expressed in the Arrhenius coordinates.

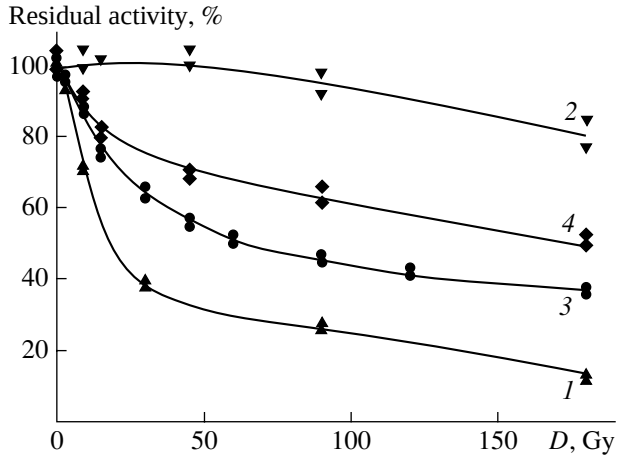

Fig. 2. The dependence of the residual activity of (*1*, *2*) somatic ACE and (*3*, *4*) ACE *N*-terminal domain on the dose of γ-irradiation (*1*, *3*) in the absence and (*2*, *4*) in the presence of ANS at the concentration of 50 mM in the mixture of 0.025 M phosphate buffer–0.025 M borate buffer (pH 6.5) containing 0.15 M NaCl and 1 μM Zn^{2+}. ACE concentration 10 nM.

was inactivated by the γ-irradiation more slowly than the somatic enzyme (Fig. 2), although its specific surface area is larger.

Radicals formed in the course of water radiolysis are known to damage first the residues of aromatic amino acids of a protein exposed to solvent [16]. On the other hand, hydrophobic regions on the protein surface can be shielded by the sorption of low-molecular compounds. Previously, we have demonstrated that one hydrophobic region capable of formation of a complex with the ANS (a hydrophobic dye) is situated on the ACE globule [17]. The ANS binding significantly protected the somatic ACE to the action of γ-radiation, and the maximum effect was achieved after the equilibrium of the complex formation was attained.

The individual *N*-domain turned out to be insignificantly stabilized in the presence of ANS (Fig. 2), which suggests that the single hydrophobic protector-binding site is in the *C*-domain of the enzyme. We should stress that the molecule of somatic ACE sensitive to radiolysis became much more stable after the formation of ANS complex than its initially more stable *N*-domain (see curves *2* and *3* in Fig. 2). These results point out to the existence of contacts between the enzyme domains, which lead to the mutual influence of the domains, including the stability toward radiolysis.

We began the analysis of possible structural differences between the domains responsible for the differences in their stability with the prediction of secondary structure of the domains of bovine ACE on the basis of the known amino acid sequence of the enzyme [18]. We predicted 45% content of the α-helical and ~50% content of unordered structure; the contribution of β-structures in the form of β-turns was insignificant (no higher than 5%). According to CD spectroscopy, 37% α-helix content is in the bovine ACE, while β-structure content is insignificant [5].

According to our model, both ACE domains have similar secondary structures in the area of their active sites. The most significant differences between the domains are observed in the relatively short regions of their *N*-terminal parts: they involve 1–105 aa in the *N*-domain and 604–705 aa in the *C*-domain (Fig. 3). The degree of homology between the *N*-terminal parts of *N*- and *C*-domains was the lowest (49%). Two amino acid insertions and four sites of potential glycosylation are present within this area of the *N*-domain, whereas the corresponding area of the *C*-domain contains three potential glycosylation sites. Moreover, it was reported in [19] that two of these four sites in the *N*-domain of

N–ACE 1 ELDPALQPGNFPADEAGAQIFAASFNSSAEQVLFQSTAASWAHDTNITEENARLQEE 57

C–ACE 604 MPDNYPEGIDLVSDEDEARKFVEEYDRRSQVVWNEYAEANWNYSTDISTDNSKLLME 661

N–ACE AALLSQEFSEAWGQKAKDLFDPVWQNFTDPTLLRIIGAVRTLGPANLD 105

C–ACE KNLQMANHTVKYGTWAS-KFD--VTNFQNATMKRMIKKIQDLERAALP 705

Fig. 3. The predicted secondary structures of the domains of bovine ACE in the regions of the largest structural differences between the *N*-domain (1–105 aa) and the *C*-domain (604–705 aa). The locations of the α-helices are underlined. The potential glycosylation sites are marked with grey boxes.

human ACE bear carbohydrate chains, whereas the corresponding region of the *C*-domain does not contain carbohydrates. The content of α-helices in the discussed region of *N*-domain is significantly higher than that in the *C*-domain (63 and 48%, respectively). This suggests that this region of the *N*-domain is more conformationally rigid. Moreover, the content of Pro residues, which should additionally increase the stability of the protein, is two times higher in the *N*-domain region.

We can presume that a higher rigidity and a higher glycosylation degree of the 1–105 region of *N*-domain and a higher flexibility of the corresponding region of the *C*-domain could probably be explained by the fact that the *C*-domain folding proceeds under the conditions when the *N*-domain has already been folded at least partially. An enhanced conformational flexibility of the initial region of the *N*-domain is necessary for the compensation of the sterical limitations associated with the presence nearby of already folded *N*-domain. This flexibility possibly results in a reduced stability of the *C*-domain we experimentally observed.

We made an attempt to model the three-dimensional structure of the two ACE domains for a more detailed description of structural differences between the domains. At the first stage, we determined the structural type of the protein folding allowed for each of the domains in accordance with their primary structures and the predicted secondary structures. It turned out that only the structure of neurolysin (35% homology with ACE) appeared to be close to both the *N*- and *C*-domains of ACE among all the protein structures known at present. Neurolysin (EC 3.4.24.16) is a zinc-dependent metalloprotease hydrolyzing short (up to 17 aa) peptides, including the well-known ACE substrates angiotensin and bradykinin, but their cleavage sites differ from the sites hydrolyzed by ACE [20]. The neurolysin polypeptide chain consists of 704 aa, which corresponds to the length of one ACE domain. The neurolysin molecule structure determined by X-ray analysis predominantly consists of α-helices (53%) and unordered structure (41%) [21]. It also includes one β-sheet comprising approximately 6% of the amino acid residues present in the protein.

Three-dimensional structures of the ACE domains were modeled on the basis of their primary structures, the models of their secondary structures, and the motif of spatial folding of the neurolysin polypeptide chain as a template (Figs. 4, 5). The model of the ACE *C*-domain was more complete, while that of its *N*-domain was limited only to the 1–477 region. This limitation was associated with the VVRNETH sequence (477–483 aa) of the *N*-domain that is crucially distinct from the LARSQDD sequence situated in the corresponding region of the *C*-domain (1075–1081 aa). As a result, the used algorithm of the model design required impermissible conformations for the side radicals of a number of amino acid residues.

Let's discuss the more complete model of the *C*-domain in detail. Practically all of the α-helices within one of the ACE domains are folded in the direction close to the location of the cleft containing the enzyme active site. The zinc-coordinating His959, His963, and Glu987 residues as well as Glu960 that participates in the polarization of the hydrolyzed peptide bond occupy positions, which make possible the catalytic reaction. The His1089 residue participating in stabilization of the catalytic transition state [22] is more than 100 amino acid residues distant from these residues, which distinguishes ACE from the other members of the zincin family. In the proposed structure, this His residue turned out to be in the common cleft with other amino acid residues of the active site. This fact confirms the correctness of our model. However, His1089 residue should be significantly closer to other residues in the real structure of the active site. Also note that His1089 is included into the long unordered loop (Fig. 4), whereas the used algorithm for the modeling of three-dimensional structure (like all other algorithms presently used) does not allow the determination of the conformation and the position of such unordered loops with sufficient accuracy.

All the Asn residues determined by Yu *et al.* [19] as subjected to glycosylation during the expression of testicular human ACE in the Chinese hamster ovary cells (Asn666, Asn685, Asn731, Asn913, and Asn1162 according the numeration in this work) are close to the surface of the ACE *C*-domain in our model (Fig. 4).

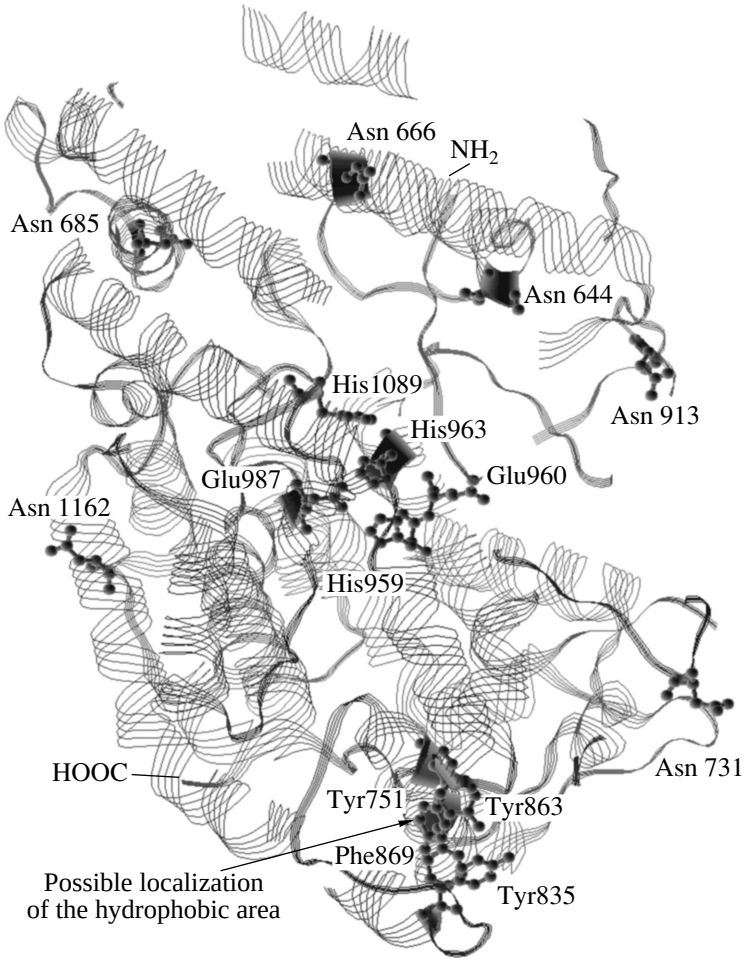

Fig. 4. The model of spatial folding of the polypeptide chain of the *C*-domain of ACE. The amino acid residues of the active site, the sites of potential glycosylation, and the amino acid residues of the proposed hydrophobic area are marked.

This fact additionally confirms the correctness of our model.

We failed to model with sufficiently high precision the *N*-terminal structures of the 1–105 sequence of the *N*-domain and of the 604–705 sequence of the *C*-domain, which we regarded as most probably responsible for different thermal stabilities of the domains. In Figures 4 and 5, one can see an incoherent protein structure with many chain breaks in these regions, which points to a low structural homology in these regions. According to the modeling results, these regions should occupy separate spatial positions. These regions are rather distant from the active sites and form structurally separate subdomains, which are probably important for the general domain stability.

The results of Marcic *et al.* [4] may confirm this conclusion: the authors prepared a chimerical human ACE with the *N*-terminal region of *C*-domain (the 601–747 sequence) replaced by the corresponding region of *N*-domain (the 1–148 sequence). This replacement affected both the catalytic properties and the stability of the mutant enzyme toward the thermal inactivation: the stability was higher than that of the *C*-domain but still lower than that of the recombinant *N*-domain.

Despite the limitations of the proposed model, it helped us find the single hydrophobic site on the surface of the ACE *C*-domain that might bind the ANS molecule and serve as a target for the damaging action of the products of water radiolysis. This hydrophobic cluster is formed by three Tyr residues (Tyr751, Tyr835, and Tyr 863) and by one Phe residue (Phe869) (Fig. 4). This hydrophobic site was rather distant from the active site cleft, which well agrees with the experimentally found fact that the ANS binding to the hydrophobic site of ACE does not affect its catalytic activity [17].

These Tyr and Phe residues are conserved and also present in the ACE *N*-domain where they, in principle, also can form a hydrophobic cluster. The fine arrangement of this cluster probably differs from that in the *C*-domain, and this difference could result in a significantly decreased binding of the dye molecule and fixing

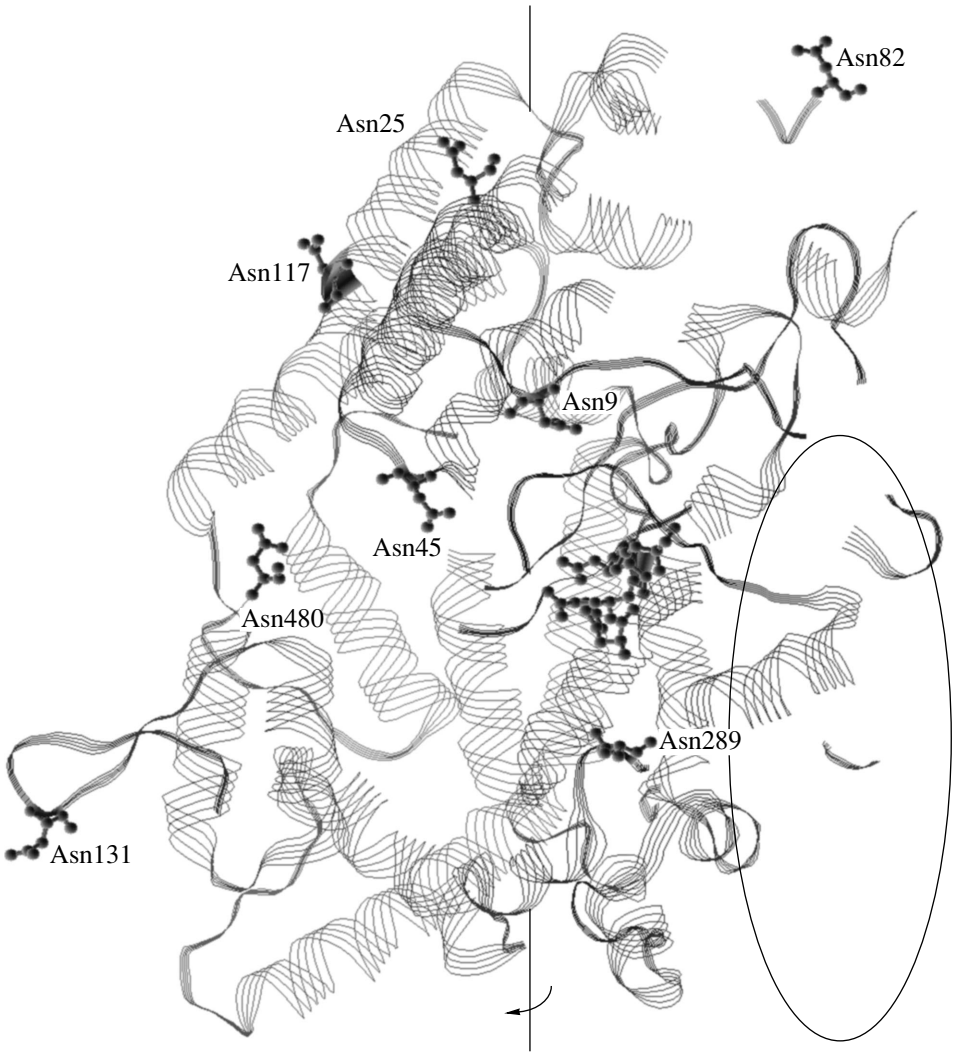

Fig. 5. The model of the spatial folding of the polypeptide chain of the *N*-domain of ACE. The amino acid residues of the active site and the potential glycosylation sites are marked. The probable carbohydrate-binding site is indicated by a circle. This projection was made from that given in Fig. 4 by a 90°-turn in the indicated direction relative to the given axis.

only one hydrophobic site on the globule of somatic enzyme under the experimental conditions.

ACE is an unusual protein, because it contains a specific carbohydrate-binding site, which imparts lectin-like properties to the enzyme [23]. The functions of this site are not associated with the direct catalytic properties of ACE, but are probably related to the structural arrangement of the enzyme in biological membrane. An analysis of the incomplete model of the enzyme *N*-domain allowed us to localize the possible region of this carbohydrate-binding site on the protein surface. It was established (O.A. Kost and S.M. Danilov, unpublished results) that the 9B9 monoclonal antibody to the *N*-domain of human ACE and its Fab-fragments shield the carbohydrate-binding site on the ACE globule and inhibit the enzyme dimerization caused by the interaction of carbohydrate chains of one enzyme molecule with the carbohydrate-binding site of the another molecule [23]. The epitope recognized by the 9B9 antibody on the surface of the somatic human ACE is situated between Lys535 and Lys572 of the ACE *N*-domain [24]. These results help localize the carbohydrate-binding site in the enzyme *N*-domain.

This region was not included in our model of the three-dimensional structure of *N*-domain. However, we presume by analogy with the homologous region of *C*-domain that this region should be situated in the space region marked by a circle in Fig. 5. It is important that the majority of the sites of potential glycosylation are situated on the same side of the ACE globule where we localized carbohydrate-binding site. Such mutual arrangement of the glycosylation sites and carbohydrate-binding site should create sterical hindrances for the carbohydrate-controlled interaction of more than two molecules simultaneously. Actually, only the formation of ACE dimers was shown to be controlled by

carbohydrates, whereas larger aggregates of the enzyme result from other interactions [25].[3]

EXPERIMENTAL

Materials. N^{α}-3-(2-Furyl)acryloyl-*L*-phenylalanyl-glycyl-glycine, *N*-(*S*-1-carboxy-3-phenylpropyl)-*L*-lysyl-*L*-proline (lisinopril), (2*S*)-1-(3-mercapto-2-methylpropionyl)-*L*-proline (captopril), and (*S*)-1-[*N*-(1-[ethyloxycarbonyl]-3-phenylpropyl)-*L*-alanyl]-*L*-proline maleate (enalapril maleate) were from Sigma (United States); hippuryl-*L*-histidyl-*L*-leucine and histidyl-*L*-leucine were from Serva (Germany); and N^{α}-benzyloxycarbonyl-*L*-phenylalanyl-*L*-histidyl-*L*-leucine was from Bachem (United States). N^{α}-3-(2-furyl)acryloyl-*L*-phenylalanyl-*L*-alanyl-*L*-alanine and N^{α}-3-(2-furyl)acryloyl-*L*-phenylalanyl-*L*-alanyl-*L*-lysine were kindly gifted by M.V. Ovchinnikov (the Cardiological Scientific Center of the Russian Academy of Medical Sciences). (*RS*)-N^{α}-[1-Carboxy-2-(benzylaminocarbonyl)ethyl]-*L*-alanyl-*L*-proline (PP-09), and N^{α}-3-(2-furyl)acryloyl-*L*-phenylalanyl-*L*-phenylalanyl-*L*-arginine were a kind gift of V.F. Pozdnev (the Institute of Biomedical Chemistry of the Russian Academy of Medical Sciences).

Somatic and testicular ACE were isolated by the method involving the enzyme extraction from bovine lungs and testes with 50 mM phosphate buffer (pH 7.5) containing 150 mM NaCl and 1 μM $ZnCl_2$ in the presence of Triton X-100 and sequential cascade affinity chromatography [26].

***N*-Domain of ACE** was prepared by a limited proteolysis of the partially denatured somatic form of ACE [5, 6].

All the preparations were homogenous according to the SDS-PAGE. The concentrations of the active ACE molecules were determined by the method of stoichiometric titration with lisinopril, a specific competitive inhibitor of the enzymatic hydrolysis, with FA-Phe-Gly-Gly substrate as described in [6].

Kinetics of the catalytic hydrolysis of FA-Phe-Gly-Gly, FA-Phe-Ala-Ala, FA-Phe-Ala-Lys, and FA-Phe-Phe-Arg were studied on a Simadzu UV-265FW spectrophotometer (Japan) by the technique [27]. The rates of catalytic hydrolysis of Hip-His-Leu and Cbz-Phe-His-Leu were measured fluorimetrically on a Hitachi MPF-4 spectrofluorimeter (Japan) by measuring the content of reaction product, His-Leu, with the use of *o*-phthalic aldehyde [28].

Determination of the inhibition constants of the single-domain forms of ACE by various competitive inhibitors was performed under the equilibrium conditions at a constant enzyme concentration and five substrate concentrations varied in the range from 0.5 to 3 × K_m. The enzyme concentration in the reaction mixture was made to be equal to K_i determined in preliminary experiments. The inhibitor concentration was varied within the range of 0.5–10 × $[E]_0$. The experimental data were processed by the Henderson method [29].

The ACE thermal inactivation was monitored by measuring the residual activity of the enzyme (with the Cbz-Phe-His-Leu substrate) after the incubation at the preset temperature for various periods of time [5]. The residual activity was calculated as percentage of the activity of the intact enzyme.

Effect of ANS on the kinetics of the radiation inactivation of ACE in the solution was studied by exposure of a 10^{-8} M solution of the enzyme to γ-irradiation [17]. The value of absorbed radiation dose was determined by the exposure time (the kinetical absorption of the dose at a constant dose rate of 0.05 Gy/s). The residual activity of the preparations was measured according to the hydrolysis rate of the Cbz-Phe-His-Leu as a substrate.

Prediction of the ACE secondary structure was performed using the Consensus service available on the Network Protein Sequence Analysis Web-server (France) http://npsa-pbil.ibcp.fr/. The structure was predicted simultaneously by eight various algorithms in which the homology with the proteins of the known crystal structures, the dependence of the conformation of an amino acid residue on its nearest environment, and the ability of an amino acid residue for the formation of hydrogen bonds were taken into account. The most probable structural conformation of every region was chosen on the basis of the results of all the prediction algorithms. The accuracy of such prediction was more than 70% according to [30].

Prediction of the motif of the spatial folding of the peptide chain of the ACE domains was carried out on the basis of the primary structures of the domains of bovine ACE using the 3D-PSSM service [31] available on the Web-server of the structural bioinformatics group of the State College of Science, Technology and Medicine (Great Britain), http://www.sbg.bio.ic.ac.uk./servers/3dpssm/.

ACKNOWLEDGMENTS

This study was partially supported by the Russian Foundation for Basic Research, project no. 00-04-482430.

REFERENCES

1. Soubrier, F., Alhenc-Gelas, F., Hubert, C., Allegrini, J., John, M., Tregear, G., and Corvol, P., *Proc. Natl. Acad. Sci. USA*, 1988, vol. 85, pp. 9386–9390.
2. Corvol, P., Williams, T.A., and Soubrier, F., *Methods Enzymol.*, 1995, vol. 248, pp. 283–305.

[3] The crystal structure of testicular human ACE was determined (Ramanathan, N., Schwager, S.L.U., Sturrok, E.D., and Acharya, K.R., *Nature*, 2003, vol. 421, pp. 551–554) when this article was accepted for publication).

3. Deddish, P.A., Wang, J., Michel, B., Morris, P.W., Davidson, N.O., Skidgel, R.A., and Erdös, E.G., *Proc. Natl. Acad. Sci. USA*, 1994, vol. 91, pp. 7807–7811.
4. Marcic, B., Deddish, P.A., Jackman, H.L., Erdös, E.G., and Tan, F., *Hypertension*, 2000, vol. 36, pp. 116–121.
5. Voronov, S., Zueva, N., Orlov, V., Arutyunyan, A., and Kost, O., *FEBS Lett.*, 2002, vol. 522, pp. 77–82.
6. Binevski, P.V., Nikol'skaya, I.I., Pozdnev, V.F., and Kost, O.A., *Biokhimiya* (Moscow), 2000, vol. 65, pp. 765–774.
7. Wei, L., Alhenc-Gelas, F., Corvol, P., and Clauser, E., *J. Biol. Chem.*, 1991, vol. 266, pp. 9002–9008.
8. Sturrock, E.D., Danilov, S.M., and Riordan, J.F., *Biochem. Biophys. Res. Commun.*, 1997, vol. 236, pp. 16–19.
9. Voronov, S.V., Binevski, P.V., Eremin, S.A., and Kost, O.A., *Biokhimiya* (Moscow), 2001, vol. 66, pp. 968–975.
10. Deddish, P.A., Wang, L.-X., Jackman, H.L., Michel, B., Wang, J., Skidgel, R.A., and Erdös, E.G., *J. Pharmacol. Exp. Ther.*, 1996, vol. 279, pp. 1582–1589.
11. Ehlers, M.R.W., Chen, Y.-N.P., and Riordan, J.F., *Biochem. Biophys. Res. Commun.*, 1992, vol. 183, pp. 199–205.
12. Danilov, S., Jaspard, E., Churakova, T., Towbin, H., Savoie, F., Wei, L., and Alhenc-Gelas, F., *J. Biol. Chem.*, 1994, vol. 269, pp. 26 806–26 814.
13. Jaspard, E., Wei, L., and Alhenc-Gelas, F., *J. Biol. Chem.*, 1993, vol. 268, pp. 9496–9503.
14. Wei, L., Clauser, E., Alhenc-Gelas, F., and Corvol, P., *J. Biol. Chem.*, 1992, vol. 267, pp. 13398–13405.
15. *Pervichnye radiobiologicheskie protsessy* (Primary Radiobiological Processes), Timofeev-Resovskii, N.V., Ed., Moscow: Atomizdat, 1973.
16. Orlova, M.A., *Usp. Khim.*, 1993, vol. 62, pp. 529–544.
17. Voronov, S.V., Skirgello, O.E., Troshina, N.N., Orlova, M.A., and Kost, O.A., *Biokhimiya* (Moscow), 2002, vol. 67, pp. 663–668.
18. Shai, S.Y., Fishel, R.S., Martin, B.M., Berk, B.C., and Bernstein, K.B., *Circ. Res.*, 1992, vol. 70, pp. 1274–1281.
19. Yu, X.C., Sturrock, E.D., Wu, Z., Biemann, K., Ehlers, M.R., and Riordan, J.F., *J. Biol. Chem.*, 1997, vol. 272, pp. 3511–3519.
20. Vincent, B., Vincent, J.P., and Checler, F., *Brain Res.*, 1996, vol. 709, pp. 51–58.
21. Brown, C.K., Madauss, K., Lian, W., Beck, M.R., Tolbert, W.D., and Rodgers, D.W., *Proc. Natl. Acad. Sci. USA*, 2001, vol. 98, pp. 3127–3132.
22. Fernandez, M., Liu, X., Wouters, M.A., Heyberger, S., and Husain, A., *J. Biol. Chem.*, 2001, vol. 276, pp. 4998–5004.
23. Kost, O.A., Bovin, N.V., Chemodanova, E.E., Nasonov, V.V., and Orth, T.A., *J. Mol. Recognit.*, 2000, vol. 13, pp. 360–369.
24. Balyasnikova, I.V., Karran, E.H., Albrecht, R.F., and Danilov, S.M., *Biochem. J.*, 2002, vol. 362, pp. 585–595.
25. Grinshtein, S.V., Levashov, A.V., and Kost, O.A., *Biokhimiya* (Moscow), 2001, vol. 66, pp. 46–54.
26. Kost, O.A., Grinshtein, S.V., Nikol'skaya, I.I., Shevchenko, A.A., and Binevskii, P.V., *Biokhimiya* (Moscow), 1997, vol. 62, pp. 375–383.
27. Holmquist, B., Bünning, P., and Riordan, J.F., *Anal. Biochem.*, 1979, vol. 95, pp. 540–549.
28. Friedland, J. and Silverstein, E., *J. Am. Clin. Pharmacol.*, 1976, vol. 66, pp. 416–424.
29. Henderson, P.J.F., *Biochem. J.*, 1972, vol. 127, pp. 321–333.
30. Deleage, G., Blanchet, C., and Geourjon, C., *Biochimie*, 1997, vol. 79, pp. 681–686.
31. Kelley, L.A., MacCallum, R.M., and Sternberg, M.J.E., *J. Mol. Biol.*, 2000, vol. 299, pp. 499–520.